AGU PUBLICATIONS

JGR

Journal of Geophysical Research: Space Physics

RESEARCH ARTICLE
10.1002/2014JA020524

Key Points:
- AP is best predicted by global SME
- The local east-west component with global SME is the best combination
- Pedersen currents are important in the current closure of discrete aurora

Correspondence to:
P. T. Newell,
patrick.newell@jhuapl.edu

Citation:
Newell, P. T., and J. W. Gjerloev (2014), Local geomagnetic indices and the prediction of auroral power, *J. Geophys. Res. Space Physics*, *119*, 9790–9803, doi:10.1002/2014JA020524.

Received 18 AUG 2014
Accepted 14 NOV 2014
Accepted article online 19 NOV 2014
Published online 11 DEC 2014

Local geomagnetic indices and the prediction of auroral power

P. T. Newell[1] and J. W. Gjerloev[1,2]

[1]The Johns Hopkins University Applied Physics Laboratory, Laurel, Maryland, USA, [2]Birkeland Centre of Excellence, University of Bergen, Bergen, Norway

Abstract The aurora has been related to magnetometer observations for centuries and to geomagnetic indices for decades. As the number of stations and data processing power increases, just how auroral power (AP) relates to geomagnetic observations becomes a more tractable question. This paper compares Polar ultraviolet imager AP observations during 1997 with a variety of indices. Local time (LT) versions of the SuperMAG auroral electrojet (*SME*) are introduced and examined, along with the corresponding upper and lower envelopes (*SMU* and *SML*). Also, the east-west component, B_E, is investigated. We also consider whether using any of the local indices is actually better at predicting local AP than a single global index. Each index is separated into 24 LT indices with a sliding 3 h magnetic local time (MLT) window. The ability to predict AP varies greatly with LT, peaking at 19:00 MLT, where about 75% of the variance (r^2) is predicted at 1 min cadence. The aurora is fairly predictable from 17:00 MLT to 04:00 MLT, roughly the region in which substorms occur. AP is poorly predicted from auroral electrojet indices from 05:00 MLT to 15:00 MLT, with the minimum at 10:00–13:00 MLT. In the region of high predictability, the local index which works best is B_E (east-west), in contrast to long-standing expectations. However, using global *SME* is better than any local index. AP is best predicted by combining global *SME* with a local index: B_E from 15:00 to 03:00 MLT and either *SMU* or *SML* from 03:00 to 15:00 MLT. In the region of the diffuse aurora, it is better to use a 30 min average than the cotemporaneous 1 min *SME* value, while from 15:00 to 02:00 MLT, the cotemporaneous 1 min *SME* works best, suggesting a more direct physical relationship with the auroral circuit. These results suggest a significant role for discrete auroral currents closing locally with Pedersen currents.

1. Introduction

A satellite image can capture much—sometimes all—of the auroral oval in a relatively short time. This makes imaging preferable for many purposes, including, when available, determining hemispheric auroral power (AP). However, such images are often not available. The images with the longest operational continuity are from Thermosphere Ionosphere Mesosphere Energetics and Dynamics (global ultraviolet imager) [*Paxton et al.*, 1999; *Zhang and Paxton*, 2008] and Special Sensor Ultraviolet Spectrographic Imager on Defense Meteorological Satellite Program (DMSP) [*Paxton et al.*, 1992]. Those images take about 20–25 min to compile, often cover only a portion of the oval, and have a repetition rate of about 101 min, none of which is conducive to studying many of the important outstanding questions about auroral dynamics.

Because of their longevity, global coverage, and high sampling rate, magnetometers have a very long tradition of serving as proxies for auroral activity. On a coarse level, *Kp* serves this purpose. Unfortunately, *Kp* has only a moderate and nonlinear correlation with AP. This was recently shown in quantitative detail [*Newell and Gjerloev*, 2011], but the limitations of *Kp* have been appreciated in a general way for much longer. Therefore, *Davis and Sugiura* [1966] introduced the auroral electrojet (*AE*) index, which is the difference between the upper (*AU*) and lower envelopes (*AL*) in the north-south component of the horizontal geomagnetic field perturbation—often called B_H, implicitly neglecting the also horizontal east-west component. Here we use a B_N, B_E, and B_z system in accordance with the notational standards of the SuperMAG project. B_N is the north-south component, and B_E is the east-west component; the latter defined positive to the east. *Davis and Sugiura* [1966] showed that periods of enhanced *AE* activity (thus, B_N perturbations in our notation) and periods of enhanced auroral activity coincided in a number of cases. For much of the last few decades, *AE* has been considered the best proxy of auroral activity, albeit with relatively little investigation of its accuracy, geophysical meaning, or the possible alternatives.

The original *AE* used just five stations. There have since been a few generalizations, the most notable of which is that *AE* is currently compiled using 12 stations. It has long been realized that using more stations would likely improve the geophysical significance of *AE*. For a few selected days, this was done at 5 min cadence [*Kamide et al*., 1982]. *Newell and Gjerloev* [2011] introduced the SuperMAG auroral electrojet (*SME*), which is conceptually *AE* but covering 100+ stations at 1 min cadence over many decades. They also showed that *SME* predicts nightside auroral power at 1 min cadence with surprising accuracy, accounting for 65% of the total premidnight AP variance (r^2). For most of this paper, we will use the latter term, namely, variance, rather than correlation coefficients, since a major goal is to predict as high a percentage of AP as possible.

In the nearly five decades, since the introduction of *AE*, the number of magnetometer stations and particularly the number of chains covering various local regions have sharply increased (e.g., the Canadian Auroral Network for the OPEN Program Unified Study chain in Canada [*Mann et al*., 2008] or International Monitor for Auroral Geomagnetic Effects (IMAGE) in Scandinavia [*Tanskanen et al*., 2011]). This naturally raises the question as to whether local versions of the *AE*, covering a specific local time range, may work better than does the global version. While intuitively reasonable, it is equally possible that the global index better predicts auroral power than do the local variations. We will show here that if a single index is used, that is, perhaps surprisingly the case, global *SME* predicts auroral power in a given magnetic local time (MLT) sector better than does any local index tested.

We here also investigate various combinations of local and global indices for their ability to predict AP. In particular, we consider *SME* upper envelope (*SMU*) and *SME* lower envelope (*SML*) as well as *SME*. The east-west component, B_E, is usually considered not to be diagnostic of AP, but as discussed in the Discussion section, the reasons for that assumption are not convincing. In addition to the standard global single value of each index, 24 local time values are also studied using a 3 h sliding window. AP observations from Polar ultraviolet imager (UVI), at 1 min cadence, are used as a diagnostic to determine which indices or combinations work best.

2. Data and Techniques

2.1. The SuperMAG *SME* (*SMU* and *SML*) Indices

Davis and Sugiura [1966] introduced the first auroral electrojet index, namely, $AE = AU - AL$. It is thought that *AU*, defined as the maximum B_N (traditionally B_H) component from any contributing station, represents the strength of the eastward auroral electrojet, primarily in the dusk cell. *AL*, defined as the lower or minimum (most negative) B_N component, represents the westward electrojet, primarily in the early morning. During substorm onset, however, the station observing the most negative B_N is usually in the dusk sector beneath the auroral expansion [e.g., *Gjerloev et al*., 2004]. Originally using 5 stations, the *AE* index has been standardized at 12 for about 40 years.

That is still a small number. Using just 12 stations to represent global dynamics is known to present problems [e.g., *Rostoker*, 1972]. *Newell and Gjerloev* [2011] used SuperMAG to introduce auroral electrojet indices at a 1 min cadence for multiple decades using up to 130 stations. Because the 12-station *AE* index is an official International Association of Geomagnetism and Aeronomy product, an alternate name, *SME* ($= SMU - SML$), is necessary for the SuperMAG version. Nonetheless, conceptually, *SME* may be regarded as *AE* (01:00 MLT). The *SME* index and ancillary data (such as the station contributing *SMU* and *SML*) are available from the SuperMAG website at 1 min cadence. An important and sometimes unappreciated aspect of index construction is the creation of a baseline. Indeed, without a baseline, interpreting perturbations is of limited value. *Gjerloev* [2012] introduced a uniform and powerful method for this necessary normalization which is applied to all data before use in the construction of the indices studied here. *SME* is calculated using all stations contributing data to the SuperMAG project and which lie in the range of 40° magnetic latitude (MLAT) through 80° MLT. Figure 1 of *Newell and Gjerloev* [2011] shows the distribution of stations used in the initial calculations, along with a comparison to the range used for standard *AE*. Unlike the official *AE*, *SME* is never finalized, as any new data added may result in recalculations.

2.2. Local Geomagnetic Indices

The LT versions of the geomagnetic indices are derived in largely the same fashion as the global values. In particular, the same filtering and baseline techniques described by *Gjerloev* [2012] are applied, along with noise removal and transformation into a common set of coordinates. The LT version of the *SMU*/*SML* envelope

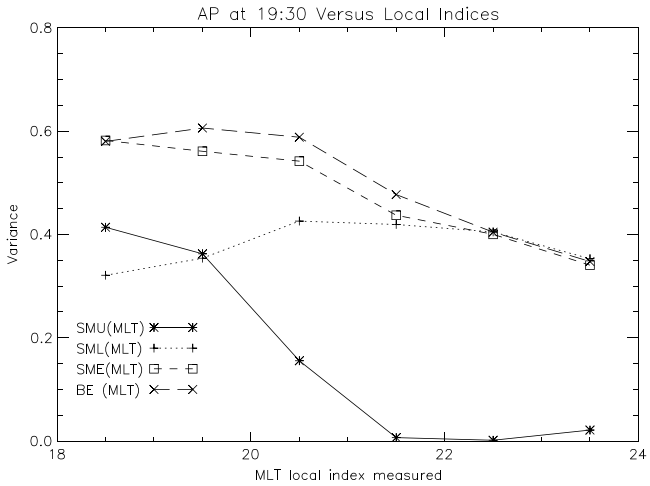

Figure 1. Polar UVI auroral power observed in 1 min images during 1997 is compared with four geomagnetic indices. The indices are calculated over a 3 h sliding window centered on each 1 h MLT step from 18:00 to 23:00 MLT. The highest correlations are observed when the local indices are also calculated at 19:00 MLT. The best choice for predicting auroral power is surprisingly the north-south perturbation, B_E (19:00 MLT).

of highest and smallest (largest negative amplitude) is calculated over a 3 h sliding window. For example, the *SMU* (00:00 MLT) index covers the range of 23:00 MLT through 02:00 MLT and is thus centered at 00:30 MLT and is defined as the largest positive B_N value in that range (meaning, the north-south component, often previously called B_H).

An additional consideration for the calculation of the local indices is a geographic restriction on contributing stations to 63° MLAT through 78° MLAT. This is still broader than the coverage of stations used in traditional *AE*. The reason for the restriction is simply that it produces significantly higher correlation with auroral power than does including polar cap or lower latitude stations.

The 3 h wide window was chosen because it was the smallest which provided a high degree of continuity, meaning that a value was computed from multiple stations in each time sector for each 1 min step. Moreover, going to smaller windows does not improve the correlations (at least in preliminary tests), probably because of the small number of contributing stations left in some bins. If the density of stations becomes high enough in the future, this issue is worth reconsidering.

2.3. B_E

Neither infinite field-aligned current sheets into the ionosphere nor longitudinal (Hall) currents through the ionosphere should give rise to an east-west (B_E) deflection, which is therefore typically ignored. If the ionosphere has a uniformly conducting surface, Fukushima's theorem [*Fukushima*, 1994] shows that, under certain geometrical assumptions, field-aligned currents do not produce a net B_E on the ground. Fringing fields of course could give rise to B_E but are unlikely to provide strong correlations—more likely would be noise or at least poor correlations. But in the absence of uniform ionospheric conductivity, as is the case in reality, local Pedersen currents can produce predictable east-west perturbations. In this study, the local largest positive component less the most negative component was subtracted in each of the 24 different 3 h windows to produce local B_E values. A global B_E was also calculated, although it has not proven to be of any particular value as it does not well predict auroral power at any local time. Similarly, the components to B_E (most positive and most negative values observed) were also correlated with AP at each local time, but also proved of little predictive value, and thus will not be further discussed.

2.4. Auroral Power From Polar UVI

Torr et al. [1995] first described the UVI on the NASA satellite Polar. UVI is a narrow-angle (8° circular field of view) imager with a large aperture (*f*/2.9). The highly eccentric orbit of Polar allowed it to monitor the northern hemisphere about 9 h out of each 18 h orbital period. Most images, including those used here, occur at 1 min cadence.

AP was calculated from the LBHL (Lyman-Birge-Hopfield long filter), centered around 170 nm. It measures molecular nitrogen lines and is relatively insensitive to the actual energy of precipitation, responding primarily to total energy flux above a few hundred eV. Ion precipitation also contributes, since it is actually the secondary electrons which stimulate the lines measured. Dayglow measurements were carefully subtracted using a normalization based on low-latitude images for each individual day. The global auroral power for the same period was computed for each LBHL image of the auroral zone according to the techniques described below.

Carbary et al. [2000] have described the technique for computing auroral power. The FUV LBH lines result almost entirely from electron impact excitation and thus are a good measure of precipitating energy flux. The LBHL filter exhibits only about a 10% variation in response as a function of the incident electron energy over the range of a few hundred eV to a few tens of keV [*Strickland et al*., 1999], wherein most incident auroral electron energy lies. The count rate observed by UVI using the LBHL filter (in units of photons/cm^2 s^{-1}, as plotted) can be converted to a nadir surface brightness in Rayleighs by multiplying by a factor of $4\pi/(\Omega 10^6) = 30.17$, where Ω is the solid angle subtended by a single pixel (4.17×10^{-7} sr). This apparent surface brightness is still convolved with the response of the LBHL filter. Off-nadir pixels are corrected by reducing the apparent brightness for the look angle by multiplying by a factor of $\cos(\theta)$, where θ is the look angle (which requires knowing the altitude of the spacecraft, and also requires an altitude for the aurora, which we assume to be 120 km). Once an apparent surface brightness, corrected for look angle, over the LBHL regime in Rayleighs is established, a conversion to incident electron energy flux is completed by use of the factor 110 Rayleighs = 1 erg/cm^2 s^{-1}. This number, which we have taken from *Brittnacher et al*. [1997], is based on modeling calculations by *Germany et al*. [1994], which in turn relies upon the calculations presented by *Strickland et al*. [1999].

The Polar UVI auroral power database was compiled by Kan Liou and has been discussed in several previous publications [e.g., *Liou et al*., 1998; *Newell et al*., 2001]. AP is integrated from 50° to 80° MLAT in each of 24 separate 1 h wide MLT bins. We used here 27,613 individual images at the intrinsic resolution of the data set, namely, 1 min. The auroral oval was also broken up into 4 sectors (00:00–06:00, 06:00–12:00, 12:00–18:00, and 18:00–24:00 MLT), and the data within any of these sectors were considered only if the entire region was within the field of view of Polar UVI.

3. Peak Local Correlations (Single Variable)

3.1. Examples From Selected Local Times

We consider now how well AP observed in a given MLT sector is correlated with selected geomagnetic indices, including locally derived indices. We will also compare AP at, say, 21:00 MLT with geomagnetic indices calculated centered around neighboring MLTs. Although intuitively, one expects that the AP observed at a given MLT is best related to geomagnetic variations occurring at that specific local time, the assumption is worth testing, especially given the zonal current flows associated with the auroral electrojets. Perhaps as importantly, checking the correlation at neighboring MLTs as well as the target MLT helps establish consistency, as will probably become clearer when specific examples are presented.

In Figure 1, the AP at 19:00 MLT over the year 1997 based on Polar UVI images at 1 min cadence is compared with indices. The geomagnetic indices have the same 1 min cadence. Thus, in Figure 1, the *x* axis is the MLT center point for computing the various indices, while the *y* axis is the variance (thus, r^2, where r is the correlation coefficient) of AP exclusively at 19:00 MLT (meaning, the 1 h bin starting at 19:00 MLT). Therefore, Figure 1 shows that using a local index centered at 19:30 MLT is—reassuringly—the best choice. More surprising is that the best local index is B_E (19:00 MLT). Less concisely but more explicitly, the east-west perturbations, or B_E, evaluated over the 3 h window centered at 19:30 MLT better predicts Polar UVI measurements of AP at 19:00 MLT than does any other local index calculated at any other local time plotted (actually better than all other local times, even those not plotted).

The next question is how these local time indices compare with using a global index. It seems reasonable to expect a locally calculated index to better predict local AP. In terms of the choice between global variables, the traditional assumption is that, in this time sector (namely, 19:00 MLT), *SMU* (or *AU*) should do better than *SME* (*AE*) and *SML* (*AL*) should have little to no predictive power. However, these assumptions do not survive when tested. The observed variances with auroral power at 19:00 MLT for the global indices are $r^2(SME) = 0.70$, $r^2(SMU) = 0.58$, and $r^2(SML) = 0.62$. In fact, the global value for *SME* outperforms not just global *SMU* (and global *SML*) but also each of the local values (including the local value of *SME*, *SME* (19:00 MLT)). Thus, to predict auroral power at 19:00 MLT by using a single magnetic index, the best choice is the global value for *SME*, while the best local value is the east-west variation (B_E), with $r^2(B_E$ 19:00 MLT$) = 0.54$.

Next consider Figure 2 showing the prediction of auroral power at 20:00 MLT from local magnetic indices. Once again, the east-west component, B_E, is the surprise winner—albeit admittedly less of a surprise the second time.

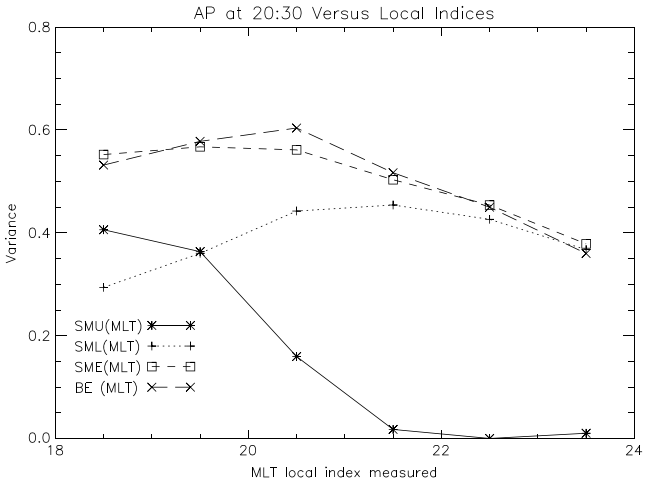

Figure 2. Same as in Figure 1 except at 20:00 MLT. The best predicting local variable is B_E (20:00 MLT).

The peak predictive power shifts to local indices centered around 20:30 MLT (the center point of the 3 h sliding window). It is a reassuring feature of virtually all 24 of these plots that the peak AP prediction at a given MLT occurs using an index also centered at that same MLT. One interesting note, however, is that for both local times considered so far, if one does wish to use a local value of *SMU* to predict AP, it is actually best to use a window centered at 18:00 MLT, rather than the MLT of the prediction target. This may be because 18:00 MLT is a bit beyond the typical region of the substorm current wedge and may therefore be more representative of an eastward electrojet.

Once again, the best single predictor is not any local index but rather the global value of *SME*. Specifically, the global indices predict variances of $r^2(SMU) = 0.55$, $r^2(SML) = 0.58$, and $r^2(SME) = 0.66$. Thus, the versatile global *SME* again outperforms the best local choice, shown in Figure 2 to be $r^2(B_E$ 20:00 MLT$) = 0.60$.

Our final case example before considering the overall pattern is for 05:00 MLT, which is shown in Figure 3. Here the results comport a bit better with classical expectations. *SML* is expected to predict auroral power best, and this is true, albeit by a modest margin. In descending order of goodness, $r^2(SML$ 05:00 MLT$) = 0.46$, $r^2(SME$ 05:00 MLT$) = 0.42$, $r^2(B_E$ 05:00 MLT$) = 0.30$, and $r^2(SMU$ 05:00 MLT$) = 0.06$. Except perhaps for the decent showing of B_E that ordering is just what is traditionally expected. The (1 min average) global indices here do a bit worse, with $r^2(SME) = 0.41$.

However, the most important characteristic to note is that the fraction of AP that can be predicted in the morning sector is significantly lower than was true premidnight. The morning sector auroral oval power is primarily diffuse aurora, while the premidnight sector power contains far more discrete aurora, as has been known for decades. Since diffuse aurora is the pitch angle scattering of the main plasma sheet population, as contrasted with the discrete aurora, which is known to be intimately associated with field-aligned currents, it seems possible that the correlation between the electrojet indices and the morningside aurora may be primarily statistical in nature. That is, both are at higher levels in geomagnetically disturbed times but without any close or causal relationship.

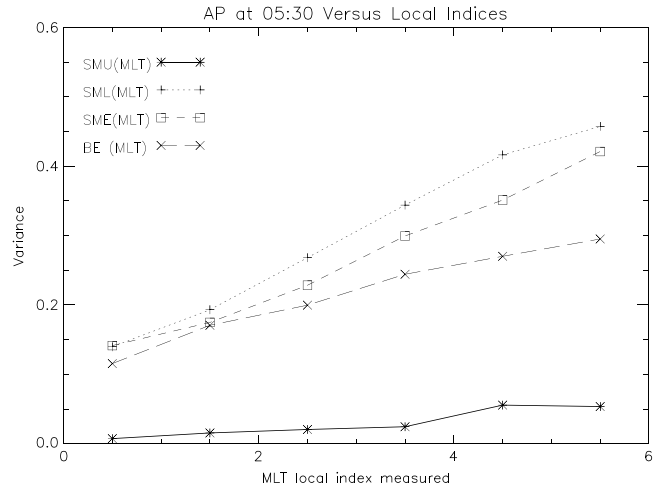

Figure 3. Same as in Figure 1 except at 05:00 MLT. In the morning sector, *SML* is the best performing local predictor of AP.

In the case of the premidnight aurora, the relationship is strongest on a 1 min cadence, meaning, when comparing each geomagnetic index to AP during that same minute. We investigated whether this was true also in the morning sector. It is not. In fact, using an average of *SME* over the 30 min which preceded the target minute proved to better predict morningside AP. At 05:00 MLT, for example, *SME* averaged over the previous 30 min predicts 46% of the AP variation ($r^2 = 0.46$), meaningfully better than the cotemporaneous

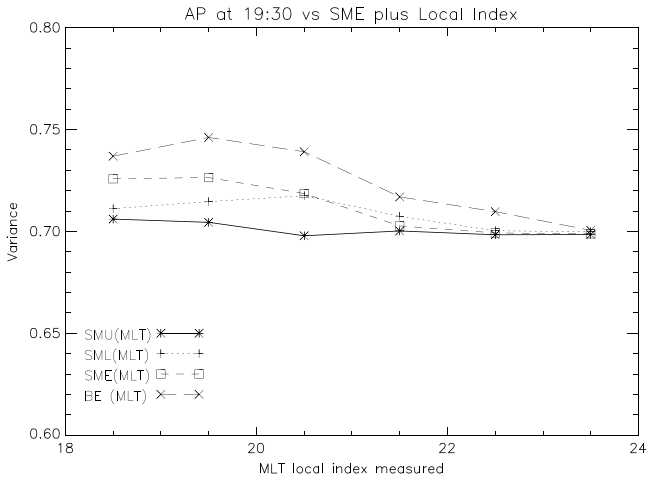

Figure 4. The variance of AP at 19:00 MLT with local indices when combined with global *SME*. The best local index to use is B_E (19:00 MLT).

1 min variance ($r^2 = 0.41$). Actually, this averaging improves the global *SME* to equal the best choice local value. In the dusk and premidnight sectors, each 1 min measurement of AP is however best predicted by the *SME* value in that same minute. Therefore, in the rest of this paper, we will continue to use the 1 min *SME* values except in the morning sector, where a 30 min average of preceding values is used.

3.2. Multivariable Correlations

If one is restricted to the use of a single variable to predict AP over the entire hemisphere, *SME* is clearly the best choice, predicting auroral variance best through most of the auroral oval. If the proviso is added that a 30 min average is used in the morning hours, *SME* equals or exceeds the choice of any global or local variable at any local time. Note that this means using a sliding 30 min window terminating at the target minute is the best predictor of the 1 min average AP in the morning sector. Specifically, global *SME* better predicts morning AP than does global *SML* (the indices traditionally assumed to be most closely related). The generalized power of global *SME*, combined with the varying ability of local time indices, suggests using a combination: global *SME* plus the best local choice.

Figure 4 shows the predictive power of various local variables when combined with global *SME* in predicting auroral power at 1 min cadence at 19:00 MLT as observed by Polar UVI. It turns out that the best local variable to use in such a combination is B_E (19:00 MLT), which was also the best choice for a single local variable. The two index combinations are amazingly powerful: a full three fourths of the auroral power variance can be predicted ($r^2 = 0.75$). The order of local variables is the same as in Figure 1, when they were considered for their single variable predictive power. This generally holds. The reason is that there is relatively modest overlap between global *SME* and the various local indices. Obviously, local B_E does not contribute to global *SME* at all, but even local *SME* does not provide the contributing global *SMU* and *SML* stations in most bins, most of the time. Thus, the local indices have a substantial independence from the global *SME* value.

Our final individual local time sample is shown in Figure 5, illustrating the predictive value of global *SME* plus one local index at 17:00 MLT. The best local variable to add to global *SME* is *SMU*, although local *SME* is nearly as good. Incidentally, the oddity in which *SMU* (16:00 MLT) better predicts auroral power at 17:00 MLT than does *SMU* (17:00 MLT) is repeated at other late afternoon sites. That is, typically, it is better to use a local *SMU* value from farther to the east than the site where auroral power is being predicted. Perhaps it is better to be a bit farther away from the region of substorms to get an accurate measure of the longitudinal eastward electrojetor perhaps the currents flowing from eastward into the target local time are more important than the currents flowing through the target local time.

3.3. Auroral Oval Power and Geomagnetic Indices: Systematics

Figure 6 shows the local index which best predicts local auroral power over the entire 24 h dial. In the early morning sector (03:00–05:00 MLT), local *SME* and local *SML* work nearly equally well, gradually transitioning to a pure *SML* dominance. Likewise, local B_E gradually gives way to local *SMU* in the afternoon sector. Overall, the major discrepancy with traditional assumptions remains the predictive ability of the east-west component (B_E) throughout most of the region of strong discrete aurora. (Many weak electron acceleration events occur around 15:00 MLT, but this does not represent a significant increase in total precipitating power [e.g., *Hardy et al*., 1985].) Another way of putting this is that throughout the region where intense aurora are associated with field-aligned currents, the local B_E component is the best local predictor of auroral power.

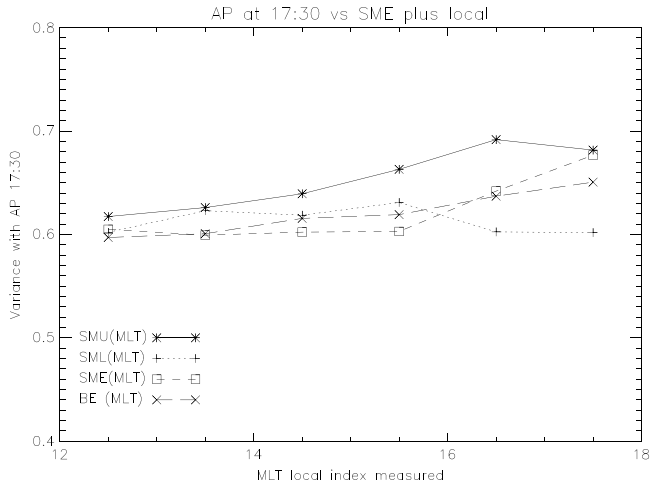

Figure 5. Same as in Figure 4 except at 17:00 MLT. The best local index to combine with global *SME* is *SMU* (16:00 MLT), that is, the eastward electrojet flowing into the region.

Figure 6 shows only which local index works best but does not illustrate the strength of the correlations. That is given in Figure 7, which shows the percentage AP (100*r^2) that is predicted using global *SME* plus the best choice local variable. Interestingly, the region over which B_E is the best choice local index is also the region over which predictive power is strongest—the exception being that using the combination of 1 min local *SML* and 30 min average global *SME* also predicts AP with good accuracy between 03:00 and 04:00 MLT. The highest predictive ability is at 19:00 MLT, when it is possible to predict about three fourths of the auroral power at a 1 min cadence by using global *SME* plus the local east-west component (B_E (19:00 MLT)). Conversely, virtually none of the AP near noon, and especially prenoon, can be predicted, even when using a combination of global and local geomagnetic indices. The region between 10:00 and 12:00 MLT in which virtually no predictive ability exists roughly corresponds to the "midday gap" of discrete aurora reported from visible light images of the auroral oval on DMSP [*Meng and Lundin*, 1986].

Although geomagnetic indices are a poor proxy for AP within the near-noon region of comparatively direct solar wind-magnetosphere coupling, it is encouraging that AP in the nightside region of internal magnetospheric dynamics can be well inferred by such indices, even at a 1 min cadence. This means that by the right choice of global plus local geomagnetic indices, substorms can be reasonably well monitored at a time resolution sufficient for many purposes.

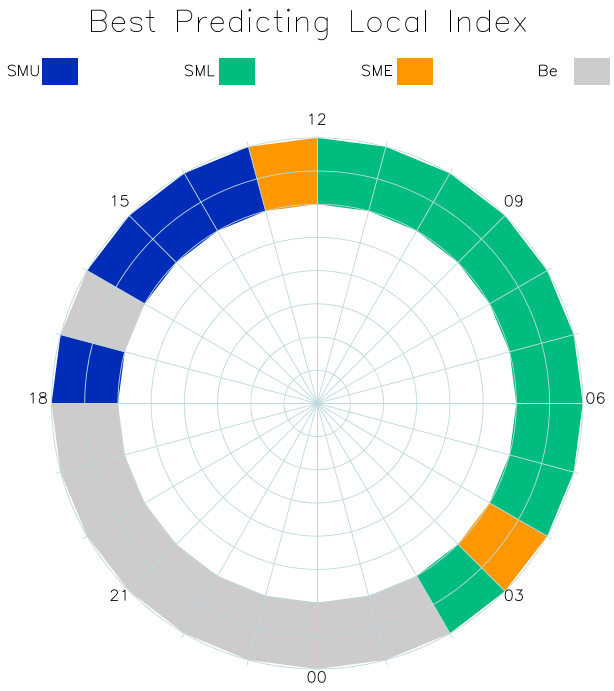

Figure 6. The best performing local index (both used alone and in combination with global *SME*) for each 1 h MLT bin.

3.4. Temporal Responsiveness

In the modern era of greatly expanded data collection and processing capability, there is a shift toward higher temporal resolution. For example, solar wind data are rarely presented on a 1 h average basis any more. Whether the best prediction of a target phenomenon comes from higher resolution or time-averaged data, however, depends on the underlying physics. For example, to use solar wind data to predict nightside AP, it is best to average over an extended time interval and include a lag. This is a result of the geophysical facts, namely, that the auroral response to the solar wind is filtered by longer-acting internal magnetospheric dynamics. For example, OVATION Prime [*Newell et al.*, 2009, 2010, 2014] would be less predictive if only the current 1 min value of the solar wind was used.

Thus, examining the temporal relationship of the aurora to the geomagnetic indices

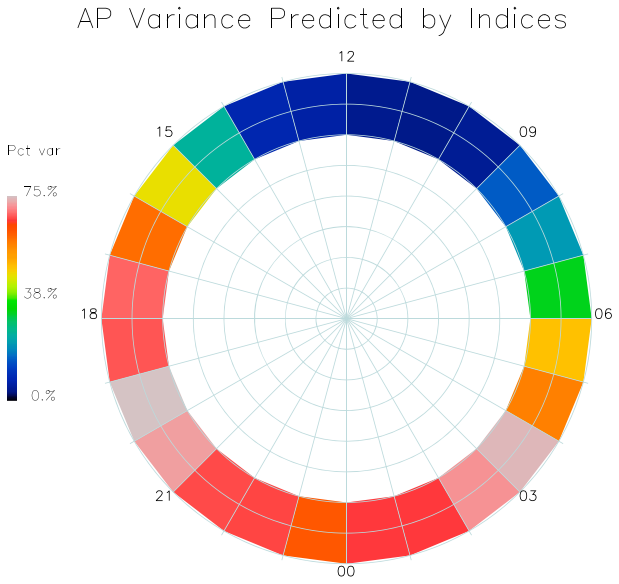

Figure 7. The fraction of AP as observed by Polar UVI at 1 min cadence that is predicted by combining global *SME* with the best performing local variable.

may help elucidate whether a direct physical connection exists. Figure 8 shows the variance of AP at 02:00 MLT, to pick an early morning example, as a function of the time lag (or lead) of the comparison measured (global) *SME* value. Figure 8 represents an attempted best prediction and therefore incorporates local B_E (evaluated at the same 1 min as the Polar UVI image providing AP). The peak variance and thus ability to predict AP occurs when *SME* is used with neither lead nor lag time. This turns out to be true throughout the auroral oval: the highest single correlation with AP is always with the indices computed over the cotemporaneous minute.

But it is not necessary to use just the current 1 min value. The next question, then, is whether it is better to use the single simultaneous 1 min value or a time average, and if the latter, averaged over how long a time. In the case of 02:00 MLT, the sharp peak in variance at the cotemporaneous minute suggests —rightly—that using just that 1 min value is best. More generally, it turns out that at some local times, it is best (most predictive) to use just the latest 1 min average, while at other local times, a running average is more predictive. After trying various possible average times (stepped in 5 min increments), a 30 min average proved to work best when averaging helped at all. The pattern of what choice to make in predicting local AP from global *SME* is not complex:

15:00 MLT – 03:00 MLT is best predicted with 1 min *SME*

03:00 MLT – 15:00 MLT is best predicted with a 30 min sliding average *SME*

Thus, the hour beginning at 02:00 MLT and ending at 03:00 MLT is best predicted with a 1 min *SME*, but the hour beginning at 03:00 MLT is best predicted with a 30 min average. For concrete examples, at 21:00 MLT, the AP variance with the cotemporaneous 1 min global *SME* is $r^2 = 0.62$ and with the 30 min average $r^2 = 0.58$. However, at 05:00 MLT, the variance with 1 min *SME* is $r^2 = 0.25$ but with the 30 min average $r^2 = 0.31$. As these examples suggest, it is largely in the region (15:00 MLT–03:00 MLT) where it is best to use just the current 1 min that the majority of AP variance can be predicted. This is what one would expect if it is auroral current circuit directly producing magnetic deflections that produces the correlation from 15:00 to 02:00 MLT. Conversely, where it is better to average over the previous 30 min, it is likely that only an indirect and likely a causual relationship exists.

4. Discussion

Before discussing the geophysical implications of our work, we briefly pause to point out Table 1, summarizing the practical results. Table 1 gives the equation best predicting AP at each local time and the percentage of 1 min AP variance predicted. This means that AP at any epoch over several decades can now be reasonably approximated by using the LT indices introduced here and soon to be available from the SuperMAG website. The formulas are all in the format

$$\mathrm{AP(MLT)} = b0 + b1^{*}(\text{best choice local variable}) + b2^{*}(\text{global } SME).$$

Thus, the fits are linear regression with two independent variables. Table 1 also specifies whether the single concurrent 1 min global *SME* or the trailing 30 min average of global *SME* is to be used (the latter is useful in the morning sector).

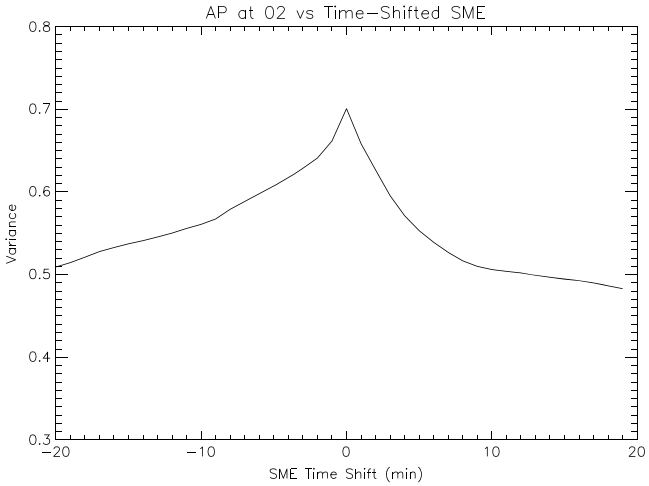

Figure 8. The variance in AP at 02:00 MLT predicted by local B_E and global *SME*, as a function of a time shift applied to *SME*. The curve is sharply peaked at $t = 0$ (no shift).

4.1. B_E and Pedersen Currents

The auroral current systems are always finite, and therefore, fringing fields exist. As long as this is true, some east-west magnetic perturbation component will always exist. *Gjerloev and Hoffman* [2014] have in fact recently discussed how field-aligned current can produce north-south perturbations on the ground. But it is difficult to see why measuring the east-west component would be more predictive than north-south component (that is, why B_E is a better predictor than B_H) if ionospheric closure currents are exclusively Hall (longitudinal) currents. Fringing fields can explain some partial correlation; it is not a satisfying explanation for why the local B_E predicts local AP better than alternative local indices. Also, the relationship between B_E and AP is quite consistent moving through a wide range of local times (e.g., consider the coefficients shown in Table 1). Therefore, it is more logical to contemplate direct means for the production of B_E from an auroral circuit.

Boström [1964], in work which likely helped inspire the creation of auroral electrojet indices, introduced the idea of "type 1" and "type 2" auroral current systems. This idea has been kept alive and considerably elaborated by Gerhard Haerendel (recent examples include *Haerendel* [2007, 2009]). Type 1 aurora closes in the ionosphere through longitudinal currents, while type 2 aurora closes through latitudinal

Table 1. Formulas Predicting AP From Linear Regression Fits Using Two Independent Variables, One Being Global *SME* (or 30 min Average *SME* Where Indicated) and the Second Being the Best Choice Local Index[a]

MLT (Start)	*b*0	*b*1	*b*2	100**r*^{2} (%)
00	0.0206	0.00765*B_E	0.00658**SME*	65.9
01	−0.0809	0.00508*B_E	0.00733**SME*	65.8
02	−0.0882	0.00312*B_E	0.00748**SME*	70.6
03	0.0347	−0.00318**SML*	0.00664* <*SME*>	73.4
04	0.676	−0.00304**SML*	0.00286* <*SME*>	57.4
05	0.989	−0.00491**SML*	0.00124* <*SME*>	46.9
06	1.17	−0.00403**SML*	0.00171* <*SME*>	32.3
07	1.22	−0.00385**SML*	0.00092* <*SME*>	20.8
08	1.20	−0.00288**SML*	0.000900* <*SME*>	14.6
09	0.978	−0.00145**SML*	0.000047* <*SME*>	4.6
10	0.865	−0.000955**SML*	0.00016* <*SME*>	3.9
11	0.790	−0.00140**SML*	0.00010* <*SME*>	4.1
12	0.597	0.000780**SMU*	0.00021* <*SME*>	6.0
13	0.622	0.00119**SMU*	0.00018* <*SME*>	8.0
14	0.654	0.00144**SMU*	0.00085* <*SME*>	24.4
15	0.509	0.00329**SMU*	0.00103* <*SME*>	45.6
16	0.286	0.00358**SMU*	0.00202**SME*	58.7
17	0.103	0.00602**SMU*	0.00243**SME*	68.2
18	0.020	0.00805*B_E	0.00280**SME*	67.0
19	−0.287	0.00845*B_E	0.00431**SME*	74.6
20	−0.190	0.0106*B_E	0.00440**SME*	71.9
21	−0.0445	0.00845*B_E	0.00550**SME*	66.6
22	−0.00127	0.0107*B_E	0.00578**SME*	66.2
23	0.104	0.00762*B_E	0.00640**SME*	61.7

[a]The formula is AP(MLT) = *b*0(MLT) + *b*1(MLT)(best local index) + *b*2*(*SME* or <*SME*>). AP is in GW. The final column gives the percentage variance predicted by the formula at 1 min cadence.

ionospheric currents (Pedersen currents). Haerendel associates type 2 aurora with pressure gradients in the equatorial plasma sheet. Although observed plasma sheet gradients are able to approximate the statistical Iijima–Potemra current patterns at least for the more poleward (*R*1) system associated with discrete aurora [cf., *Wing and Newell*, 2000; *Iijima and Potemra*, 1978], there is no reason to expect all substorm-related currents, or more generally, all monoenergetic aurora to correspond to such equatorial gradients.

Figure 9 shows a type 2 auroral circuit. Although *Haerendel* [2007] has stressed currents arising from pressure gradients in the magnetotail, any field-aligned currents can produce aurora (e.g., those associated with substorm-induced currents). The north-south or Pedersen currents give rise to east-west deflections and thus will be observed as local B_E. The connection between the strength of the B_E deflection and the currents is direct, and likewise auroral power is known to be closely related to the strength of field-aligned currents, on both a theoretical [e.g., *Lyons*, 1980] and observational [*Wing et al*., 2011] bases.

The reader may recall Fukushima's theorem [for example, *Fukushima*, 1994], which, among other things, demonstrates that in geometries similar to the auroral ionosphere (flat or spherical), field-aligned currents above a uniform conducting plane will not produce any net east-west deflection on the ground. The geometrical deviations from the assumptions of the Fukushima theorem do not strike us as profound, but the deviations from a uniformly conducting surface in the ionosphere do. In fact, the nightside auroral precipitation, which creates most of the nightside conductivity, is highly irregular, with large patches of darkness (as anyone who has examined many global images is aware). *Fukushima* [1994] himself pointed out that field-aligned currents do produce east-west deflections above the ionosphere. Without a uniformly conducting surface, they will do so below as well.

In any event, large east-west magnetic perturbations are observed on the ground. This is an observational fact. It is the proper job of theorist to explain why not to explain why it should not be so.

4.2. Four Zones: The Predictability Pattern

The overall pattern of how predictable AP is from geomagnetic indices can be divided into four zones. First, near midnight, or more concretely, from 20:00 MLT to 02:00 MLT, about 60–67% of the 1 min AP variations are predictable. This is very good. Yet on wings, extending further near dusk or dawn (19:00–21:00 MLT and 02:00–04:00 MLT), the auroral predictability is even higher, a surprising 70–75%. Thus, predictability actually rises a bit in the initial move away from midnight in either direction.

AP predictability drops moving further toward noon, so that both the morning and afternoon sectors have a lower predictability, generally roughly around half the minute-to-minute variation or modestly less. The fourth and final zone lies between 08:00 and 14:00 MLT. AP variations cannot be significantly predicted using geomagnetic indices or at least not as developed here.

As a whole, the discrete aurora, which peaks (in AP) premidnight, is more predictable than is the diffuse aurora. Diffuse aurora has been generally assumed to be less dynamic and probably more predictable, as a direct dumping of the plasma sheet. However, at 19:00 MLT, where an amazing 75% of the variance in AP can be predicted at a 1 min cadence from local plus global geomagnetic indices, discrete aurora is a large fraction of the total. The combination of the local B_E plus the global *SME* is quite powerful in this range. The modest reduction in predictability close to midnight may reflect a variety of discontinuities. The Harang discontinuity, the change in the Iijima–Potemra statistical current pattern, and the complexity of the near-midnight field-aligned current behavior [e.g., *Ohtani et al*., 2010] are all possibly involved.

The poor predictability of dayside AP is a bit disappointing. It has long been appreciated that the stations contributing to global *SMU* and *SML* (or at least *AU* and *AL*) are almost always on the nightside [e.g., *Gjerloev et al*., 2004]. Therefore, it is not too surprising that global *SME* is a poor predictor of dayside AP. However, the use of local indices seemed a plausible way to improve this deficit. This is not the case, as even with local indices, dayside AP is largely unpredictable, at least from the use of geomagnetic indices related to the auroral electrojets.

Still, most of hemispheric AP can be reasonably well predicted. It is worth keeping in mind that on a hemispheric basis, nightside power is much more significant than dayside [*Hardy et al*., 1985]. This is especially true during

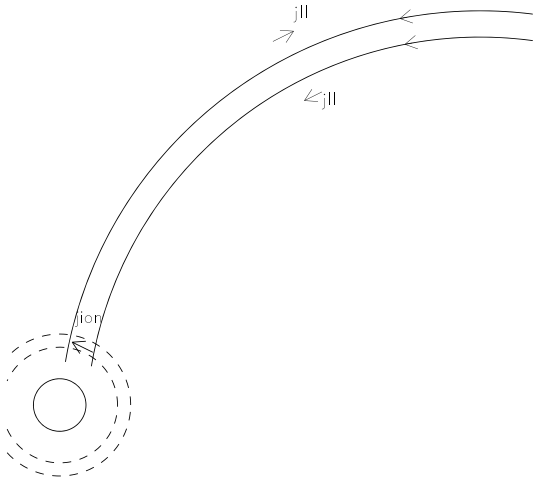

Figure 9. Auroral circuit for type 2 aurora, with local Pedersen currents closing the field-aligned currents.

disturbed intervals. For example, in a superposed analysis study using Polar UVI, dayside AP dissipated totaled 70.7 TJ in the 2 h following a substorm versus a nightside total of 152.4 TJ averaged over 390 substorms [*Newell et al.*, 2001].

4.3. Dayglow Contamination Issue

A simple, albeit wrong, explanation for the low predictability of AP near noon needs to be discussed. The Lyman-Birge-Hopfield lines measured by Polar UVI are subject to dayglow contamination. Of course, this dayglow is uncorrelated with AP and thus with the auroral electrojet.

In fact, removal of dayglow was treated with great carefulness by Kan Liou, who compiled this AP database. Specifically, instead of using generic corrections based on $F_{10.7}$ and look angle, he considered each day individually, finding an instance of low-latitude glow that could not be aurora, and used this specifically to calibrate dayglow for just that single day. There are rather good reasons to believe that the method was successful. Extensive studies of the effects of UV insolation on aurora have been done using both DMSP and Polar UVI [*Newell et al.*, 1996, 1998; *Liou et al.*, 2001; *Shue et al.*, 2001]. There is a good agreement on how UV insolation affects the dayside aurora between these two data sets, which does not seem possible if dayglow was not properly removed.

It is however true that ionospheric conductivity from sunlight has a significant effect on the currents flowing in the ionosphere and hence the perturbations measured. Roughly speaking, stronger perturbations are observed beneath a conducting ionosphere, other things being equal. The indices are prepared without any explicit conductivity considerations. It may be that a careful alteration of the indices adjusting them for observational conditions would make the indices more predictive on the dayside. We point out, however, the dawn-dusk asymmetry, in which the dusk sector (with discrete aurora) is much better predicted using indices than is the dawn sector (which consists of diffuse aurora drifting eastward from the nightside plasma sheet). Therefore, we argue that the main reason the dayside AP is not predictable from auroral electrojet indices is that this precipitation is in fact largely independent of those currents.

4.4. Local Versus Global Indices and Substorm Onsets

In terms of predicting total AP in a given 1 h MLT bin, we have shown here that global *SME* is better than using a localized version of *SME* (or *AE*). Also, although it is usually assumed that *AU* better represents auroral power near dusk and *AL* near dawn, actually *AE* (or better *SME*) best predicts total auroral power. This seems to imply limited use for *AL* and especially for the localized versions of *AL* such as the IMAGE chain *IL* [*Tanskanen et al.*, 2011] for Scandinavia.

However, the situation is a bit more complicated. For the specific purposes of identifying substorms, we also found that the traditional preference for *AL* (or *SML* or other variant) was well justified. Specifically, in terms of ability to match substorm onset times as identified by Polar UVI, *SML* outperforms *SME* [*Newell and Gjerloev*, 2011]. How can this be reconciled with *SME* outperforming *SML* in predicting total auroral power? The reason is that an auroral breakup associated with substorm onset is, for the first couple of minutes at any rate, highly localized and initially only a minority of the auroral power. It is indeed best identified by a rapid change in *SML* rather than absolute magnitudes of AP (*SME*). Since the auroral breakup is both a localized phenomenon—at first possibly only seen by a single station—and a minority of AP, it is not a contradiction to state that total AP is best predicted by the magnitude of *SME*; yet the first signs of onset are identified by a rapid change in *SML*.

Thus, for the specific purpose of identifying substorm onsets, the introduction and use of a local *IL* over Scandinavia [*Tanskanen et al.*, 2011] is indeed justified, as is consistent with the practical experience of many researchers.

4.5. Does the Dusk-Midnight AP Vary Synchronously?

AP correlates best with global *SME* in the 16:00–02:00 MLT sector (if just one local or global index is to be used). At first consideration, this seems to imply that all these areas change AP roughly synchronously, that is, as *SME* changes. In fact, the nowcast approach developed by *Evans* [1987] implicitly assumed such a relationship, since the technique uses AP along one trajectory to infer AP for the whole hemisphere. The current results suggest that this approach probably works best if the single pass used occurs in the 16:00–02:00 MLT region and if this is also the target region being predicted.

Still, the correlations from just using *SME* alone are not all that high, for example, $r = 0.70$ at 19:00 MLT and 0.66 at 20:00 MLT. The variances corresponding to higher correlations shown on Figure 7 include combining global *SME* and the best choice local index. Strictly speaking, then, we can only infer a correlation between 19:00 MLT and 20:00 MLT of at least 0.70*0.66, or 0.46, with $r^2 = 0.21$. Therefore, one can predict at least a fifth of the AP variance at 20:00 MLT from measuring AP at 19:00 MLT. Actually, 19:00 and 20:00 MLT almost certainly have higher mutual correlations than the minimum implied by their mutual correlation with global *SME*. Explicitly investigating the cross correlation of AP at different local times is a possible source of interesting future work.

5. Summary and Conclusions

With a rising number of magnetometer stations and increases in computational power, there is naturally interest in the extent to which the general idea of auroral electrojet indices can be made more precise. Specifically, it is logical to consider whether local magnetometer observations or global indices best predict local AP and which constituent parts of the magnetometer observations are most indicative at varying local times. Perhaps more fundamentally, without understanding how the magnetic observations relate to AP, our ability to understand the auroral current circuit is constrained. Here we considered in each of 24 sliding MLT windows the relationship between AP as measured by Polar UVI and several possible local and global geomagnetic indices, as evaluated at 1 min cadence.

One clear result of this study is that the utility and significance of global *SME* are confirmed. In most cases, global *SME* works better than a regional version of *SME* even if one wishes to predict AP just in that region. *SME* is also more powerful than its constituent parts. Despite the putative association of *SMU* with dusk aurora and *SML* with dawn, AP in both regions is better predicted by global *SME*. Thus, we recommend global *SME* to be used as the index of choice when AP is to be predicted on the basis of a single index.

One can still consider which of the possible local indices works best in a given MLT sector. Alternately, one can consider which local or global variables one should combine with *SME* to better predict local AP. Happily, at any given local time, both questions turn out to have the same answer. For example, throughout a very broad swath (18:00–03:00 MLT), the best local variable is the east-west deflection, B_E, and the latter is also the best choice to combine with global *SME* to predict local AP. In the region where substorms occur, it is possible to predict—perhaps reconstruct would be more accurate—a large majority of AP variance at 1 min cadence by combining global *SME* with local B_E. Essentially, this means that combining a global measure of the longitudinal ionospheric currents with a local measure of latitudinal currents is the best choice to predict local AP within the region of strong discrete aurora.

The ability to predict AP drops as one moves more than a few hours from midnight, especially in the morning sector. Since the AP in this sector is mostly diffuse aurora, and largely results from electron curvature and gradient drifting from the nightside, it is perhaps understandable if disappointing that the predictability drops. The relationship to ionospheric currents is apparently weaker, and so far as it does exists, it may be more of a general association (most aspects of geomagnetic disturbance increase together) than a specific physical connection. The fact that in the morning sector, it is better to use a 30 min average *SME* than the single cotemporaneous 1 min *SME* lends further support to the more indirect association between the indices and diffuse AP.

Nearer to noon, AP is virtually independent of geomagnetic indices, and thus cannot be reconstructed by this means, even using local indices restricted to the dayside. Perhaps the problem is that in this region, there is more direct coupling to the solar wind and the less direct coupling to the internal magnetospheric dynamics.

Predicting or reconstructing AP as accurately as possible is largely a practical issue. However, these results are strongly suggestive of a rather basic result about the auroral circuit. The local superiority of B_E from 15:00 MLT to 02:00 MLT, along with the preference for using the cotemporaneous 1 min value in this region, together with the high predictability, are all consistent with a type 2 auroral circuit configuration, in which Pedersen currents close at least a portion of the local auroral activity. All this occurs within the region of strong discrete aurora including the substorm bulge. Therefore, the present results suggest that local discrete AP is directly connected to both the global auroral electrojet strength and the local Pedersen current.

Acknowledgments

This work was supported by NSF grants AGS-1353825, AGS-1132361, and ANT-1043010. K. Liou developed the Polar UVI auroral power database, and provided it to us back in 2000, and it has proven immensely useful ever since. The following PIs contributed data helping constitute the *SME* index: J.J. Love, I. Mann, K. Yumoto and K. Shiokawa, D. Boteler, S. McMillan, M. Moldwin, E. Tanskanen, C. Stolle, P. Chi, SPIDR/NOAA, O. Troshichev, M. Engebretson, UCLA/IGPP and Florida Institute of Technology, F. Honary, M. Conners, DTU Space, and IZMIRAN. Data access statement: The SuperMAG website (http://supermag.jhuapl.edu/) provides most data used here. The global indices are already available there, and the local versions will soon follow. The Polar UVI auroral power data only exist for 1997 and are available on a case-by-case basis from Kan Liou (Kan.Liou@jhuapl.edu).

Alan Roger thanks Ramon Lopez and another reviewer for their assistance in evaluating this paper.

References

Boström, R. (1964), A model of the auroral electrojets, *J. Geophys. Res.*, *69*, 4983–4999, doi:10.1029/JZ069i023p04983.

Brittnacher, M., R. Elsen, G. Parks, L. Chen, G. Germany, and J. Spann (1997), A dayside auroral energy deposition case study using the Polar Ultraviolet Imager, *Geophys. Res. Lett.*, *24*, 991.

Carbary, J. F., K. Liou, A. T. Y. Lui, P. T. Newell, and C.-I. Meng (2000), "Blob" analysis of auroral substorm dynamics, *J. Geophys. Res.*, *105*, 16,083–16,091, doi:10.1029/1999JA000210.

Davis, T. N., and M. Sugiura (1966), Auroral electrojet activity index AE and its universal time variations, *J. Geophys. Res.*, *71*, 785–801, doi:10.1029/JZ071i003p00785.

Evans, D. S. (1987), Global statistical patterns of auroral phenomena, in *Quantitative Modeling of Magnetospheric-Ionospheric Coupling Processes*, edited by Y. Kamide and R. A. Wolf, Kyoto Sangyo Univ., Japan.

Fukushima, N. (1994), Some topics and historical episodes in geomagnetism and aeronomy, *J. Geophys. Res.*, *99*(A10), 19,113–19,142, doi:10.1029/94JA00102.

Germany, G. A., M. R. Torr, D. G. Torr, and P. G. Richards (1994), Use of FUV auroral emissions as diagnostic indicators, *J. Geophys. Res.*, *99*, 383.

Gjerloev, J. W. (2012), The SuperMAG data processing technique, *J. Geophys. Res.*, *117*, A09213, doi:10.1029/2012JA017683.

Gjerloev, J. W., and R. A. Hoffman (2014), The large-scale current system during auroral substorms, *J. Geophys. Res. Space Physics*, *119*, 4591–4606, doi:10.1002/2013JA019176.

Gjerloev, J. W., R. A. Hoffman, M. M. Friel, L. A. Frank, and J. B. Sigwarth (2004), Substorm behavior of the auroral electrojet indices, *Ann. Geophys.*, *22*, 2135–2149.

Haerendel, G. (2007), Auroral arcs as sites of magnetic stress release, *J. Geophys. Res.*, *112*, A09214, doi:10.1029/2007JA012378.

Haerendel, G. (2009), Poleward arcs of the auroral oval during substorms and the inner edge of the plasma sheet, *J. Geophys. Res.*, *114*, A06214, doi:10.1029/2009JA014138.

Hardy, D. A., M. S. Gussenhoven, and E. Holeman (1985), A statistical model of auroral electron precipitation, *J. Geophys. Res.*, *90*, 4229–4248, doi:10.1029/JA090iA05p04229.

Iijima, T., and T. A. Potemra (1978), Large-scale characteristics of field-aligned currents associated with substorms, *J. Geophys. Res.*, *83*, 599–615, doi:10.1029/JA083iA02p00599.

Kamide, Y., et al. (1982), Global distribution of ionospheric and field-aligned currents during substorms as determined from six IMS meridian chains of magnetometers: Initial results, *J. Geophys. Res.*, *87*, 8228–8240, doi:10.1029/JA087iA10p08228.

Liou, K., P. T. Newell, C.-I. Meng, M. Brittnacher, and G. Parks (1998), Characteristics of the solar wind controlled auroral emissions, *J. Geophys. Res.*, *103*, 17,543–17,557, doi:10.1029/98JA01388.

Liou, K., P. T. Newell, and C.-I. Meng (2001), Seasonal effects on auroral particle acceleration and precipitation, *J. Geophys. Res.*, *106*, 553–5542, doi:10.1029/1999JA000391.

Lyons, L. R. (1980), Generation of large-scale regions of auroral currents, electric field potentials, and precipitation by the divergence of the convection electric field, *J. Geophys. Res.*, *85*, 17–24, doi:10.1029/JA085iA01p00017.

Mann, I. R., et al. (2008), The Upgraded CARISMA Magnetometer array in the THEMIS Era, *Space Sci. Rev.*, *141*, 413–451, doi:10.1007/s11214-008-9457-6.

Meng, C.-I., and R. Lundin (1986), Auroral morphology of the midday oval, *J. Geophys. Res.*, *91*, 1572–1584, doi:10.1029/JA091iA02p01572.

Newell, P. T., and J. W. Gjerloev (2011), Evaluation of SuperMAG auroral electrojet indices as indicators of substorms and auroral power, *J. Geophys. Res.*, *116*, A12211, doi:10.1029/2011JA016779.

Newell, P. T., C.-I. Meng, and K. M. Lyons (1996), Discrete aurorae are suppressed in sunlight, *Nature*, *381*, 766–767.

Newell, P. T., C.-I. Meng, and S. Wing (1998), Relation to solar activity of intense aurorae in sunlight and darkness, *Nature*, *393*, 342–344.

Newell, P. T., K. Liou, T. Sotirelis, and C.-I. Meng (2001), Auroral precipitation power during substorms: A Polar UVI Imager-based superposed epoch analysis, *J. Geophys. Res.*, *106*(A12), 28,885–28,896, doi:10.1029/2000JA000428.

Newell, P. T., T. Sotirelis, and S. Wing (2009), Diffuse, monoenergetic, and broadband aurora: The global precipitation budget, *J. Geophys. Res.*, *114*, A09207, doi:10.1029/2009JA014326.

Newell, P. T., T. Sotirelis, and S. Wing (2010), Seasonal variations in diffuse, monoenergetic, and broadband aurora, *J. Geophys. Res.*, *115*, A03216, doi:10.1029/2009JA014805.

Newell, P. T., K. Liou, Y. Zhang, T. Sotirelis, L. J. Paxton, and E. J. Mitchell (2014), OVATION Prime-2013: Extension of Auroral Precipitation Model to Higher Disturbance Levels, *Space Weather*, *12*, doi:10.1002/2014SW001056.

Ohtani, S., S. Wing, P. T. Newell, and T. Higuchi (2010), Locations of night-side precipitation boundaries relative to R2 and R1 currents, *J. Geophys. Res.*, *115*, A10233, doi:10.1029/2010JA015444.

Paxton, L. J., et al. (1999), Global ultraviolet imager (GUVI): Measuring composition and energy inputs for NASA Thermosphere Ionosphere Mesosphere Energetics and Dynamics (TIMED) mission, *Proc. Soc. Photo-Optical Instrum. Eng. (SPIE)*, *3756*, 265–276, doi:10.1117/12.366380.

Paxton, L. J., C.-I. Meng, G. H. Fountain, B. S. Ogorzalek, E. H. Darlington, J. Goldsten, and K. Peacock (1992), SSUSI: Horizon-to-horizon and limb-viewing spectrographic imager for remote sensing of environmental parameters, *Ultraviolet Technology IV, SPIE*, *1764*, 161–176.

Rostoker, G. (1972), Geomagnetic indices, *Rev. Geophys. Space Phys.*, *10*, 935–950.

Shue, J.-H., P. T. Newell, K. Liou, and C.-I. Meng (2001), The quantitative relationship between auroral brightness and solar EUV Pedersen conductance, *J. Geophys. Res.*, *106*, 5883–5894, doi:10.1029/2000JA003002.

Strickland, D. J., J. Bishop, J. S. Evans, T. Majeed, P. M. Shen, R. J. Cox, R. Link, and R. E. Huffman (1999), Atmospheric ultraviolet radiance integrated code (AURIC): Theory, software architecture, inputs, and selected results, *J. Quant. Spectrosc. Radiat. Transfer*, *62*, 689–742.

Tanskanen, E. I., T. I. Pulkinnen, A. Viljanen, K. Mursula, N. Partamies, and J. A. Slavin (2011), From space weather toward space climate time scales: Substorm analysis from 1993 to 2008, *J. Geophys. Res.*, *116*, A00134, doi:10.1029/2010JA015788.

Torr, M. R., et al. (1995), A far ultraviolet imager for the international solar-terrestrial physics mission, *Space Sci. Rev.*, *71*, 329.

Wing, S., and P. T. Newell (2000), Quiet time plasma sheet ion pressure contribution to Birkeland currents, *J. Geophys. Res.*, *105*, 7793–7802, doi:10.1029/1999JA900464.

Wing, S., S.-I. Ohtani, J. R. Johnson, M. Echim, P. T. Newell, T. Higuchi, G. Ueno, and G. R. Wilson (2011), Solar wind driving of dayside field-aligned currents, *J. Geophys. Res.*, *116*, A08208, doi:10.1029/2011JA016579.

Zhang, Y., and L. J. Paxton (2008), An empirical Kp-dependent global auroral model based on TIMED/GUVI FUV data, *J. Atmos. Sol. Terr. Phys.*, *70*, 1231–1242, doi:10.1016/j.jastp.2008.03.008.